Supporting Information

Balancing Transesterification Reactivity of Isosorbide with Diphenyl

Carbonate: Preferential Activation of *exo*-OH

Ming Zhang, Yifei Tu, Zibo Zhou and Guozhang Wu*

Shanghai Key Laboratory of Advanced Polymeric Materials, School of Materials Science &

Engineering, East China University of Science & Technology, Shanghai 200237, China

Corresponding Author *E-mail: wgz@ecust.edu.cn

1. Standard curves of Ph-OH and DPC

The standard curve of Ph-OH was obtained as shown in Figure S1a, and the fitted

equation $y = 31471 + 1.17 \times 10^9 x$ exhibited an excellent linear relation in the

concentration range of 1.8×10^{-5}–7.0×10^{-3} g/mL. The solution concentration of

Ph-OH (C_{Ph-OH}) calculated by the standard curve was converted to the melt

concentration of Ph-OH (C_p) in the reaction system according to Eq. (S1):

$$C_p = \frac{C_{Ph-OH} \times (M_{ISB} + M_{DPC})}{C_o \times M_{Ph-OH} \times (V_{ISB} + V_{DPC})},$$ (S1)

where, the C_o = 0.01 g/mL, which was the concentration of the extracted melt

acetonitrile solution. The molar mass of ISB (M_{ISB}), M_{DPC} and M_{Ph-OH} was 146.1, 214.2,

and 94.1 g/mol, respectively. The molar volume of ISB (V_{ISB}) and V_{DPC} was 99.0 and

178.9 cm³/mol.

The standard curve of DPC was shown in Figure S1b, and the fitted equation

$y = 33385 + 8.12 \times 10^8 x$ appeared an excellent linear relation in the concentration

range of 2.2×10^{-5}–7.0×10^{-3} g/mL. Then the melt concentration of DPC (C_d) was

obtained by Eq. (S2) based on the solution concentration of DPC (C_{DPC}):

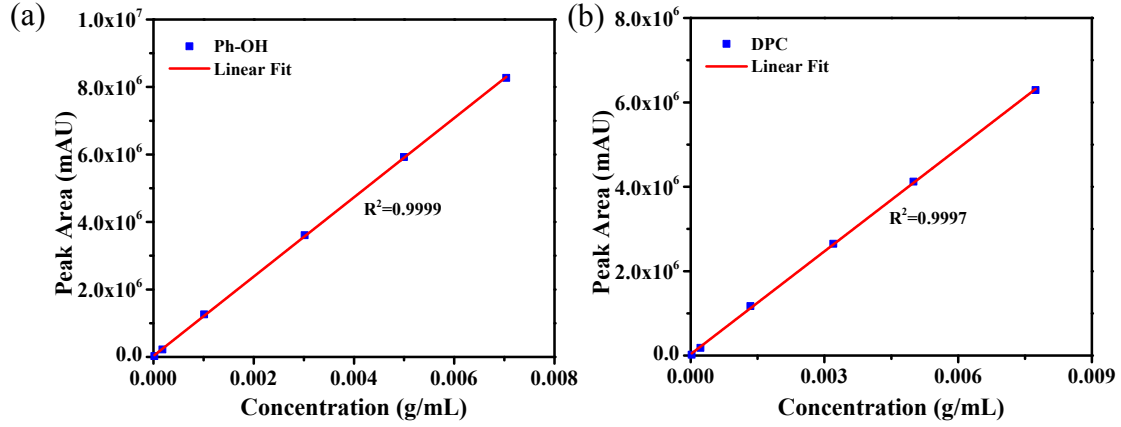$$C_d = \frac{C_{DPC} \times (M_{ISB} + M_{DPC})}{C_o \times M_{DPC} \times (V_{ISB} + V_{DPC})},$$ (S2)

Figure S1. The standard curve of (a) PhOH and (b) DPC

2. Determination of K, k^+ and k^-

According to the Bi *et al.*,[1] the reaction rate (r) can be expressed as follows:

$$r = \frac{d[P]}{dt} = k^+[A][B] - k^-[C][P]$$

(S3)

where: [A], [B], [C] and [P] represented respectively the current concentrations of -OH group, phenyl carbonate group, ISB-PC repeating unit and Ph-OH. k^+ and k^- were respectively the inherent forward and backward reaction rate constants, and t was time.

The reagents were added at equimolar ratio, and the consumptions were the same for A and B, so $[A] = [B] = [A]_0 - [P]$ and [P] = [C] at any time. When the reaction did not reach an equilibrium, r can be expressed by the [P]:

$$r = \frac{d[P]}{dt} = k^+([A]_0 - [P])^2 - k^-[P]^2$$

(S4)

At equilibrium, $\frac{d[P]}{dt} = 0$, the equilibrium constant K can be expressed as follows:

$$K = \frac{k^+}{k^-} = \frac{[P]_e^2}{([A]_0 - [P]_e)^2}$$

(S5)

where $[P]_e$ was the equilibrium concentration of Ph-OH.

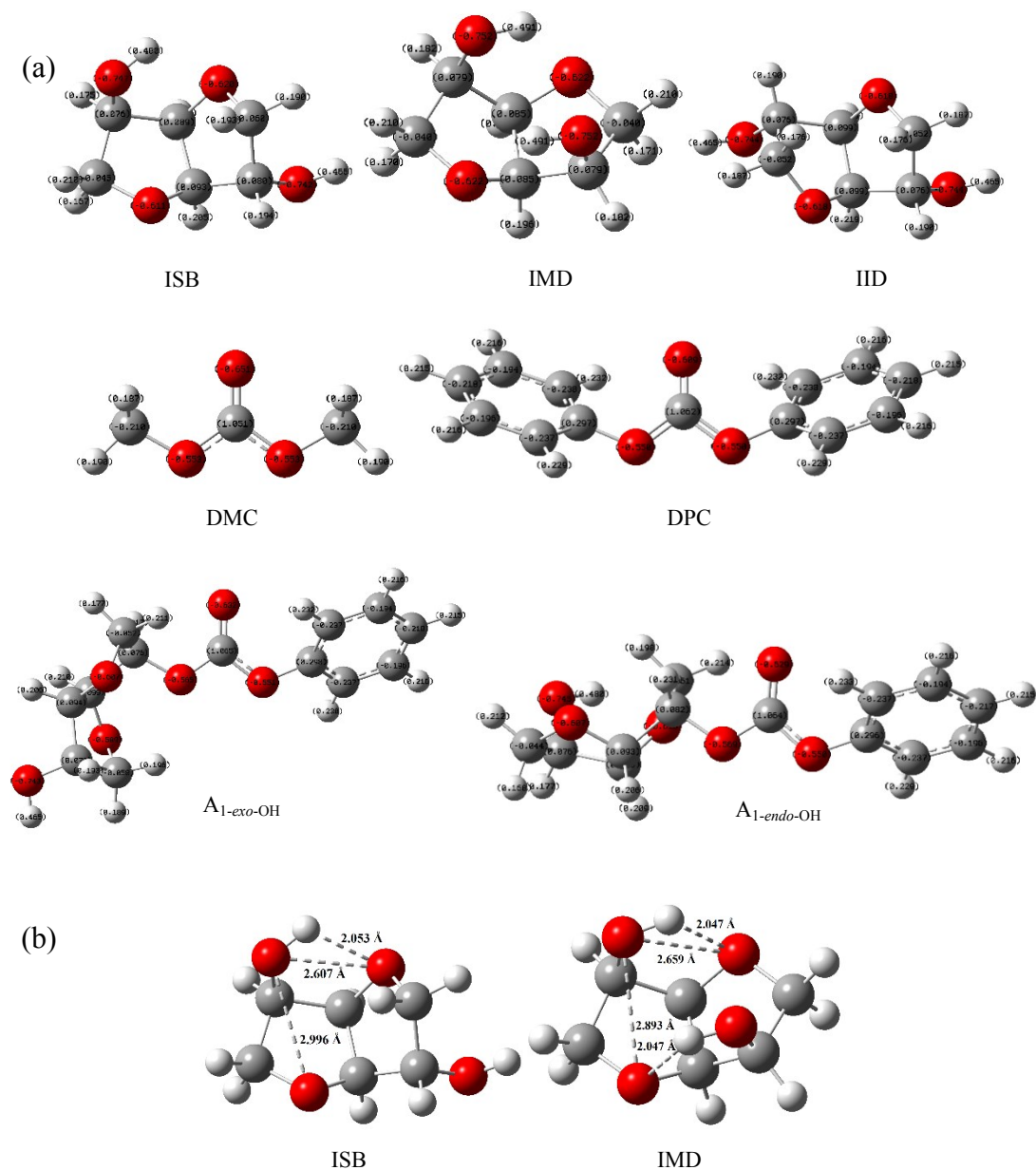Based on the Eqs. (S4) and (S5), the r can be expresses as follows:

$$r = \frac{d[P]}{dt} = k^+([A]_0 - [P])^2 - \frac{k^+}{K}[P]^2$$

(S6)

Then k^+ can be expressed further by integrating:

$$Y = \frac{\sqrt{K}ln[([A]_0 - [P] + [P]/\sqrt{K})/([A]_0 - [P] - [P]/\sqrt{K})]}{2[A]_0} = k^+t$$

(S7)

The left-hand side of Eq. (S7) was regarded Y, which was linearly related to the t.

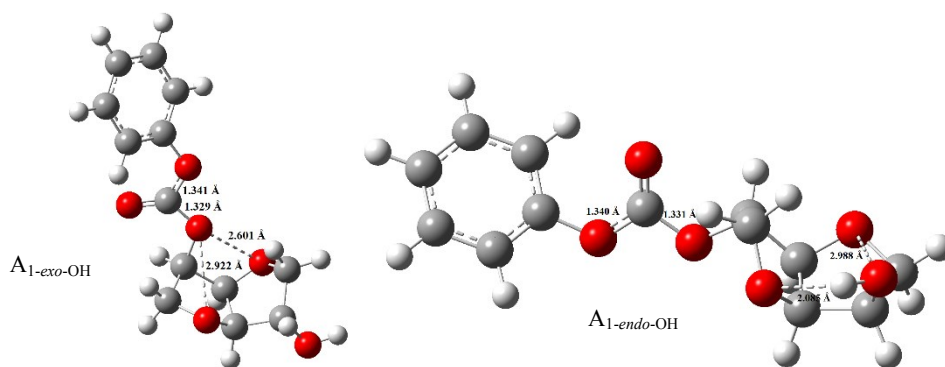## 3. NBO atomic charge distribution and selected bond lengths

(a)

ISB   IMD   IID

DMC   DPC

A$_{1\text{-}exo\text{-}OH}$ A$_{1\text{-}endo\text{-}OH}$

(b)

ISB   IMD

Figure S2. (a) NBO atomic charge distribution and (b) selected bond lengths
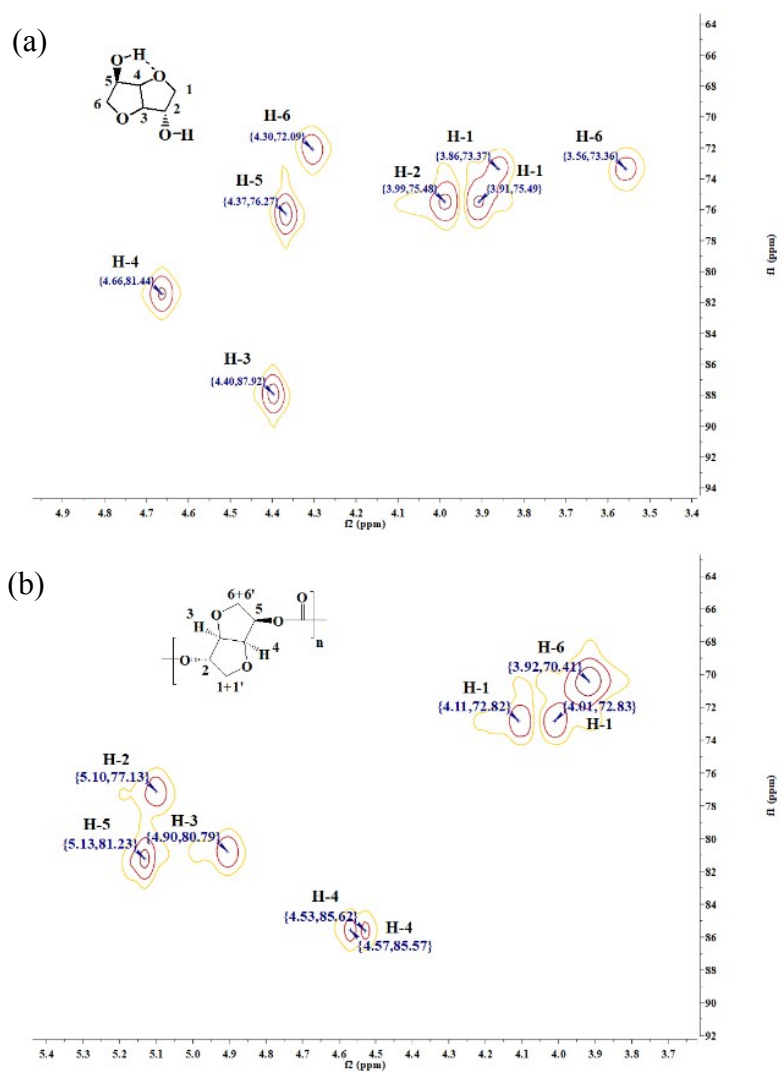
4. The assignment of proton peak in ^{1}H NMR

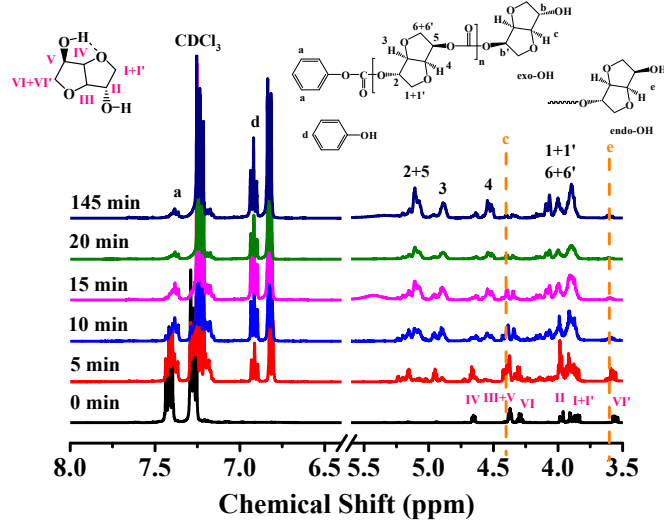**Figure S3.** HMQC spectra of (a) ISB and (b) ISB-PC oligomer

Figure S4. The ^{1}H NMR spectra of oligomers catalyzed by LiOH

According to the previous literatures,[2-4] HMQC spectra of the ISB and ISB-PC oligomer were given as shown in Figure S3, and thus the assignment of relative proton peak in ^{1}H NMR was affirmed (Figure S4). The peaks at δ4.06, 5.10, 4.90, 4.55, 5.13, and 3.92 ppm were assigned to hydrogen atoms recorded as 1, 2, 3, 4, 5, and 6 of ISB-PC repeating unit, respectively. The peaks at δ3.88, 3.99, 4.40, 4.66, 4.37, and 3.56 (4.30) ppm were assigned to hydrogen atoms recorded as I, II, III, IV, V, and VI of ISB, respectively. In addition, the peaks at δ4.40 and 3.60 ppm were respectively assigned to terminal *exo*-OH and *endo*-OH of ISB-PC oligomer.

It was apparently observed that the 'III' and 'V' peaks of ISB is overlapping with the 'c' peak of oligomer, while the 'VI' is approaching to the 'e' in the initial stage of transesterification in Figure S4. To calculate accurately the contents of terminal -OHs, the overlapping ISB was subtracted according to the Eqs. (S8) and (S9):

$$C_{exo-OH} = (I_{exo-OH} - 2 \times \frac{I_{exo-OH} + I_{endo-OH} - I_{Ph-OH}}{3})/I_{IV} , \quad (S8)$$

$$C_{endo-OH} = (I_{endo-OH} - \frac{I_{exo-OH} + I_{endo-OH} - I_{Ph-OH}}{3})/I_{IV} , \quad (S9)$$

where, C_{exo-OH} and $C_{endo-OH}$ were respectively the content of terminal *exo*-OH and *endo*-OH. I_{exo-OH} and $I_{endo-OH}$ represented the integration of peaks at δ4.40-4.37

ppm and δ3.60-3.56 ppm, and I_{Ph-OH} and I_{IV} were the integration of 'd' and 'IV' peaks, respectively.

5. The assignment of signal peak in GC-MS

According to the MS in Figure S7, the assignment of the signal peaks in Figure 4 can be affirmed except 5 and 6 by comparing with data in the NIST MS library. Because the molar mass was the 266.1 g/mol, signals 5 and 6 were believed as the $A_{1-endo-OH}$ and $A_{1-exo-OH}$. It was reported that the intermolecular hydrogen bonding of terminal *exo*-OH can raises the boiling point.[5] Therefore, the peak 5 was regard as the $A_{1-endo-OH}$ and peak 6 was $A_{1-exo-OH}$.

The GC-MS spectrum of melt catalyzed by KOH for 5 min at 160 °C was shown in Figure S5. Signals 7 and 8 were regarded as the $A_{2-endo-OH}$ and $A_{2-exo-OH}$ with the molar mass of 438.1 g/mol. Notably, it was observed that the abundance of signal peak 5 was similar to that of signal 6, and peak 7 was similar to peak 8, which were consistent with the narrowest disparity of two terminal -OH contents at the critical time as shown in Figure 6, further to confirm the above the conclusion.

In addition, the only peak was detectable at the middle position between $A_{1-endo-OH}$ and $A_{1-exo-OH}$ in GC-MS spectra of the IMD-PC oligomer (Figure S6), and it was identified as A_1 of IMD-PC with 266.1 g/mol.
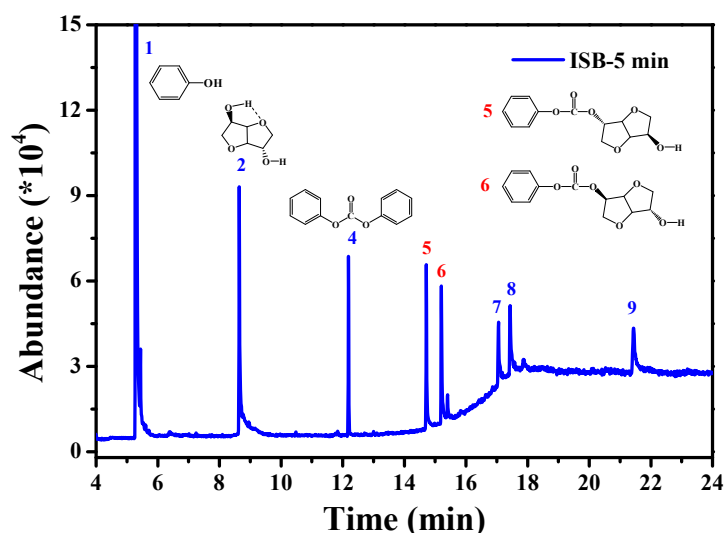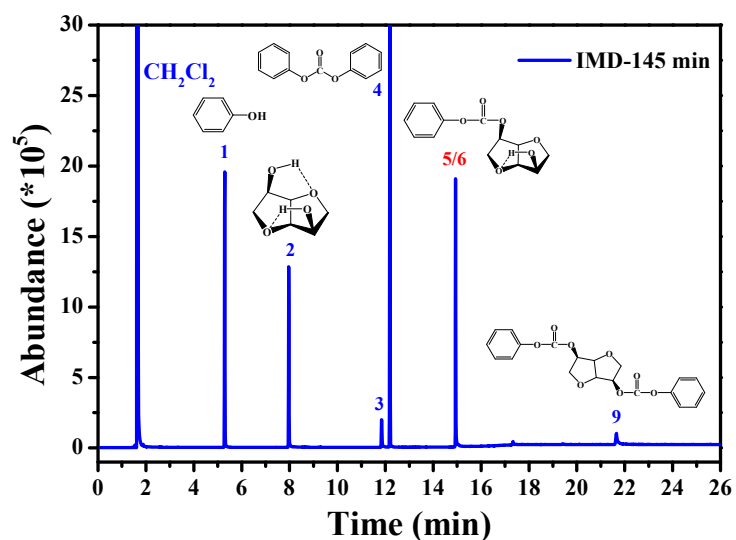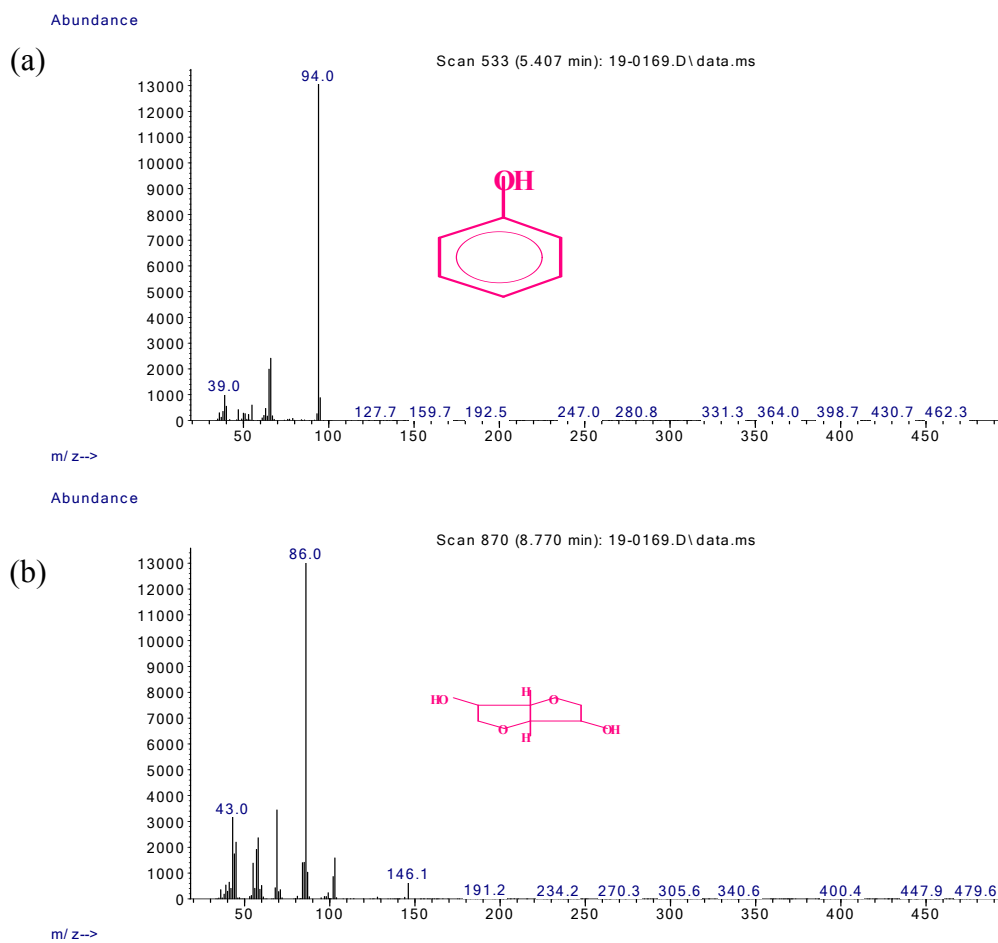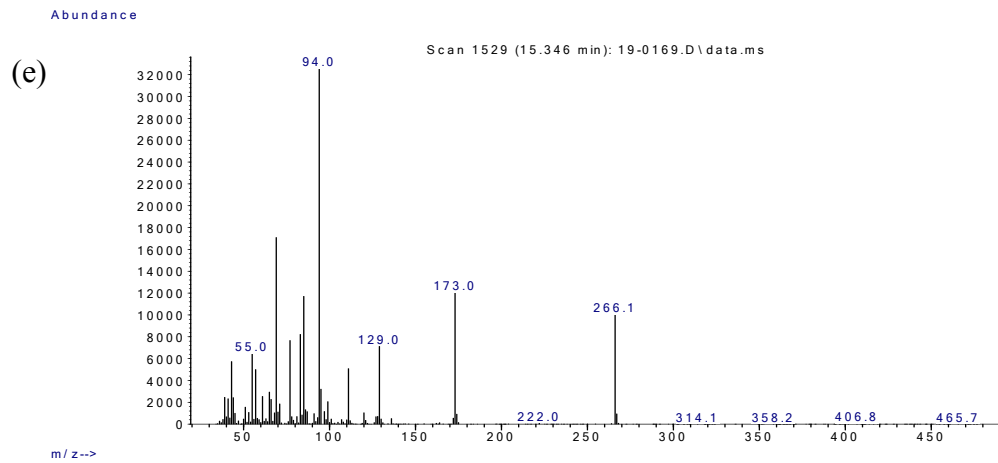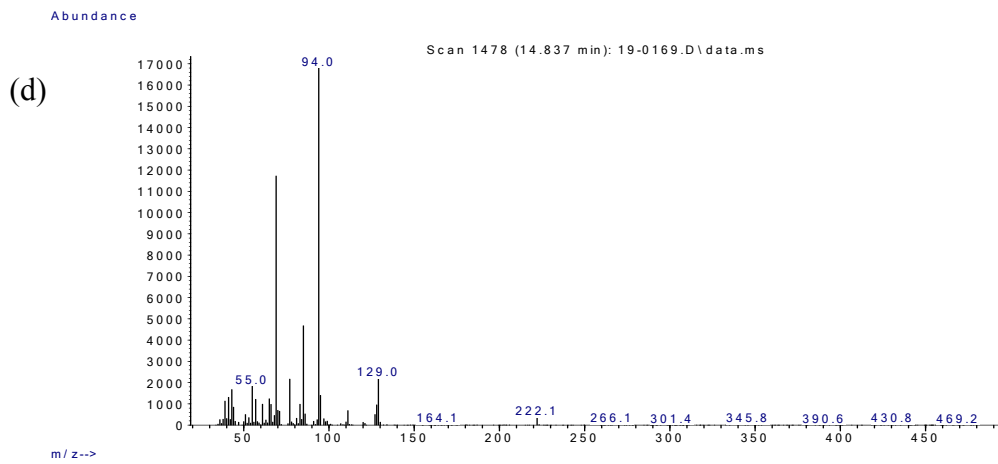

Figure S5. The GC-MS spectra of the reaction melt obtained by KOH using ISB at 160 °C for 5 min

Figure S6. The GC-MS spectra of the reaction melt using IMD without catalysts at 160 °C for 145 min

Abundance

(a)

Scan 533 (5.407 min): 19-0169.D\data.ms

m/z-->

Abundance

(b)

Scan 870 (8.770 min): 19-0169.D\data.ms

m/z-->

(c)

Scan 1224 (12.303 min): 19-0169.D\data.ms

214.1
141.1
77.0
39.0
175.2   248.7   284.3   326.7   388.3   420.6   465.9

m/z-->

(d)

Scan 1478 (14.837 min): 19-0169.D\data.ms

94.0
55.0
129.0
164.1   222.1   266.1   301.4   345.8   390.6   430.8   469.2

m/z-->

(e)

Scan 1529 (15.346 min): 19-0169.D\data.ms

94.0
173.0
266.1
55.0
129.0
222.0   314.1   358.2   406.8   465.7

m/z-->

(f)

(g)
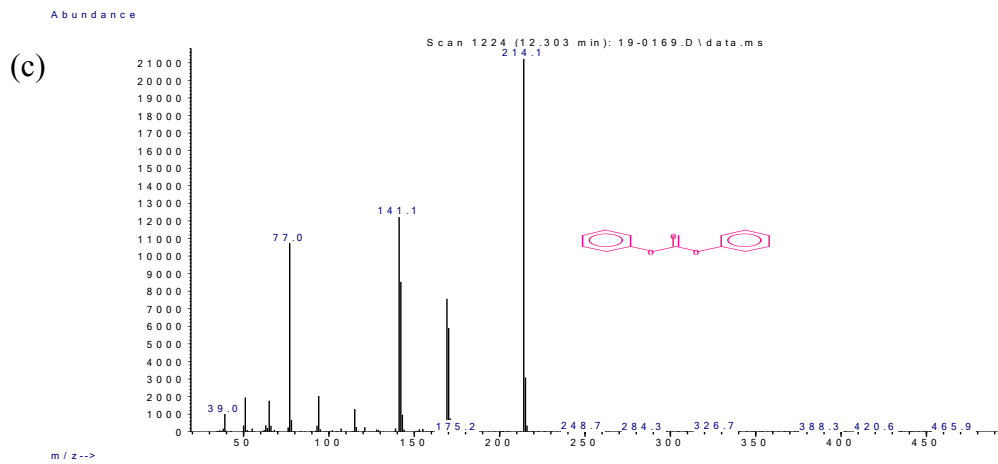
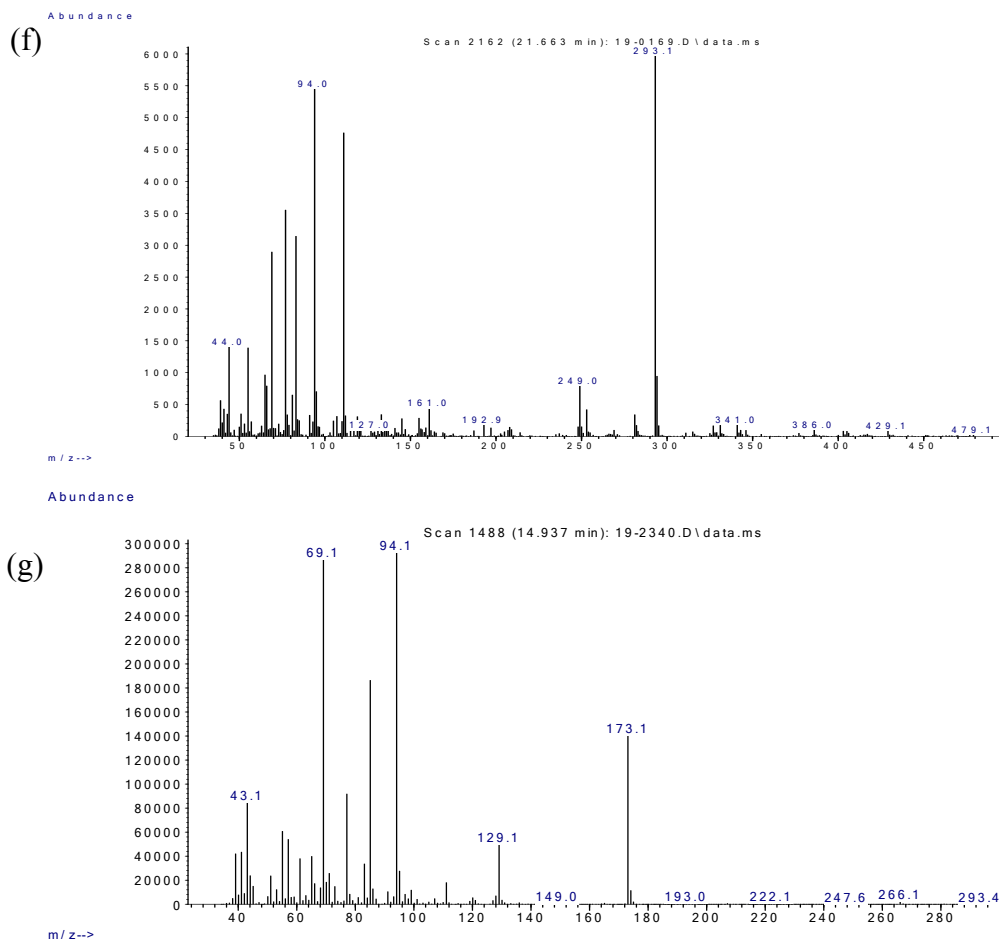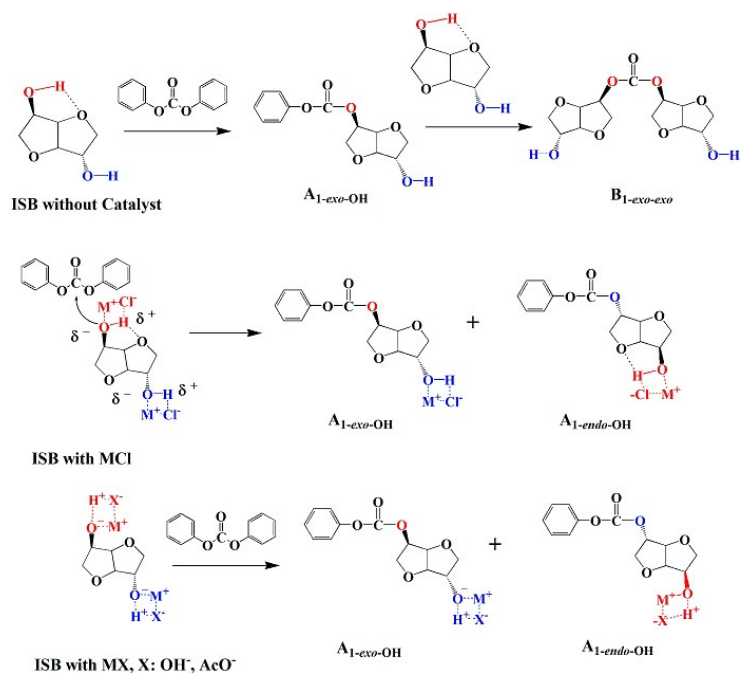**Figure S7.** MS spectra of (a-f) peaks 1, 2, 4, 5, 6 and 9 in Figure S5 and (g) peak 5/6 in Figure S6

7. The probable catalytic mechanism

Scheme S1. The probable catalytic mechanism of transesterification between ISB and DPC

7. Activation energy and reaction heat of transesterification

The activation energy (E) was determined by the Arrhenius equation (S10) and by simplifying as in Eq. (S11):

$$k = Ae^{-\frac{E}{RT}},$$ (S10)

$$lnk = \frac{-E}{RT} + lnA,$$ (S11)

where, k was the reaction rate constant, A was an exponential factor that is a constant for a given chemical reaction, R was the universal gas constant and T was the absolute temperature.

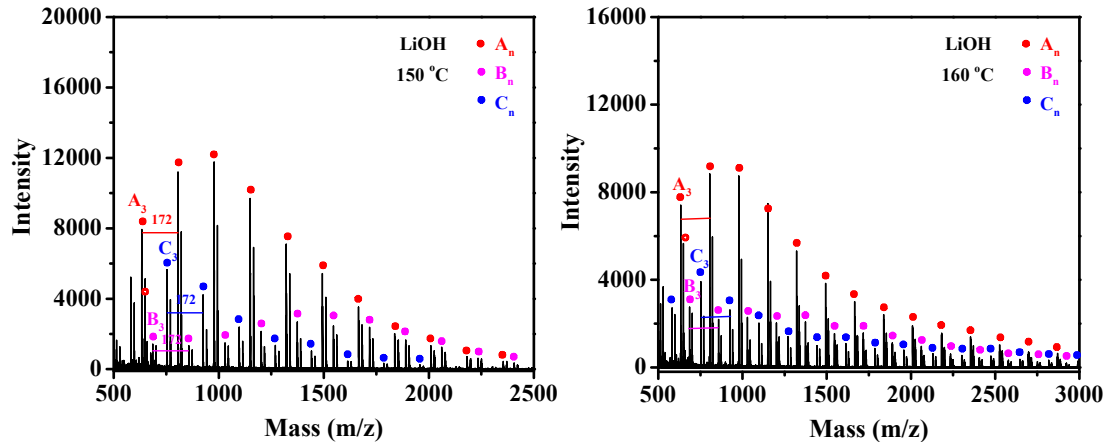The apparent reaction enthalpy (ΔH_m^θ) was calculated by the Van't Hoff equation (S12) and by integration as in Eq. (S13):

$$\frac{dlnK}{dT} = \frac{\Delta H_m^\theta}{RT^2},$$ (S12)

$$lnK = -\frac{\Delta H_m^\theta}{RT} + c,$$ (S13)

where, K was the equilibrium constant and c was constant.

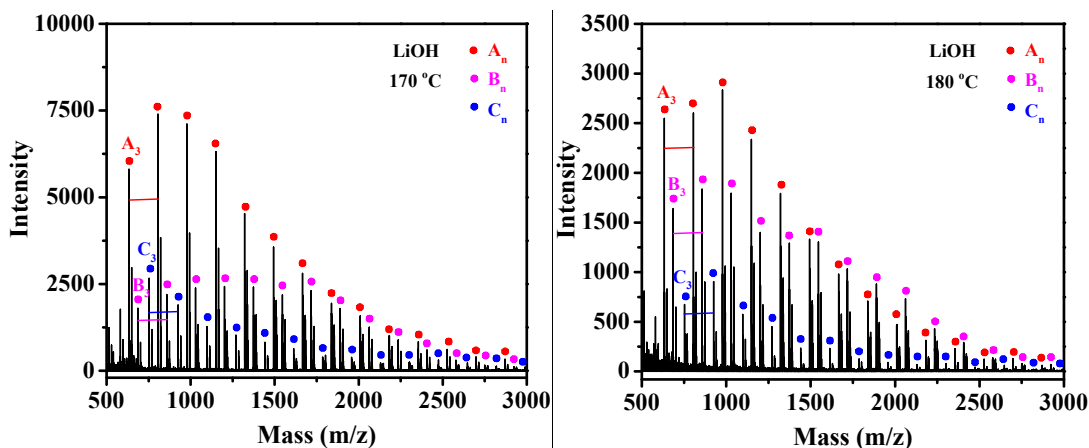## 8. The MALDI-TOF spectra of oligomers catalyzed by LiOH for 55 min at different temperatures

Figure S8. The MALDI-TOF spectra of oligomers catalyzed by LiOH for 55 min at different temperatures

9. Chemical structure and M_n of oligomers catalyzed by LiOH

Table S1. Chemical structure and M_n of oligomers catalyzed by LiOH for 55 min at different temperatures

Entry	T (°C)	Ph-OH[a]	exo/endo[a]	A_n[b] (%)	B_n[b] (%)	C_n[b] (%)	M_n (g/mol)[b]	PDI[b]
1	150	1.62	1.16	56.67	22.71	20.62	1198	1.21
2	160	1.56	0.67	55.32	22.91	21.77	1354	1.32
3	170	1.66	0.68	50.00	28.87	21.13	1359	1.36
4	180	1.53	0.78	42.55	39.87	17.57	1259	1.27

[a] determined by ^{1}H NMR analysis; [b] calculated from MALDI-TOF

10. Preparation of the high-performance isosorbide polycarbonate

ISB-PCs were synthesized from the transesterification oligomers through the melt polycondensation with the removal of phenol under vacuum as shown in Table S2. It was found that ISB-PCs cannot be obtained by NaCl and KCl because many unreacted monomers were pumped away at high vacuum. Although KOH and NaOH exhibited the high catalytic activity, the molecular weight of synthesized ISB-PCs was low

relatively. The probable reason was difficult to largely consume the low reactive terminal *endo*-OHs during the polycondensation stage. *Exo/endo* of oligomers and the molecular weight of ISB-PCs were correlated as shown in Figure S9 (pink dot data from our previous work[6]) and listed in Table S2. The results clearly illustrated that *exo/endo* of oligomer was controlled to be close 1 by activating appropriately ISB's *exo*-OH, which was advantageous to improve significantly the molecular weight of ISB-PC. The high molecular weight beyond 36,000 g/mol was achieved by Ca(AcO)$_2$ and Mg(AcO)$_2$ in this work.
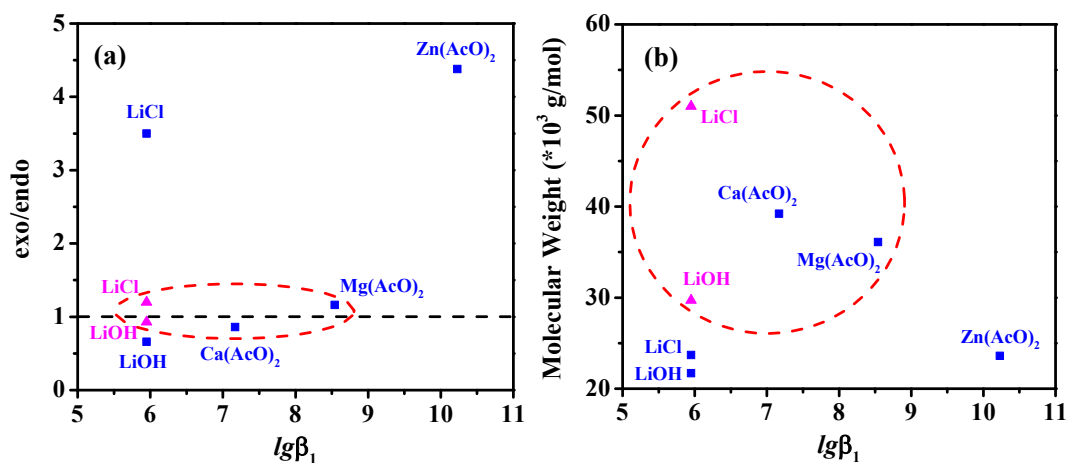

Figure S9. (a) *Exo/endo* of oligomers and (b) molecular weight of ISB-PCs prepared by the optimized catalysts

A number of *endo-endo* structure on ISB-PC molecular chain was beneficial to improve the T_g.[7-10] In this study, it was found that the reactivity of ISB's *endo*-OH catalyzed by LiCl, Ca(AcO)$_2$, Mg(AcO)$_2$ and Zn(AcO)$_2$ was much higher than *exo*-OH resulted from a large ratio of *exo/endo* in the oligomer, thereby increasing the *endo-endo* content ($a_1/a_3 > 1$) to improve the T_g of high-molecular-weight ISB-PC as shown in Table S2. The low T_g of ISB-PC catalyzed Zn(AcO)$_2$ was probably attributed to the hydrolysis of ISB moiety during the prolonged transesterification reaction.[7,11,12]

Table S2. Molecular weight, chemical structure and thermal property of ISB-PCs

Entry	Catalyst	*exo/endo*[a]	Conversion of DPC (%)[b]	–OH	a_1	a_1/a_3	$[\eta]$	M_η (g/mol)	T_g (ºC)
1	KOH	0.64	99.1	0.05	0.48	0.87	26.41	13,100	128
2	NaOH	0.65	99.1	0.04	0.47	0.96	31.84	16,500	154
3	LiOH	0.66	99.1	0.02	0.45	0.98	39.90	21,700	155
4	Ca(AcO)$_2$	0.86	98.9	0.01	0.49	1.05	64.90	39,200	166
5	Mg(AcO)$_2$	1.16	98.5	0.01	0.49	1.07	60.62	36,100	167

6	Zn(AcO)$_2$	4.38	95.1	0.02	0.52	1.02	42.77	23,600	162
7	KCl	3.68	61.8	-	-	-	-	-	-
8	NaCl	59.30	55.1	-	-	-	-	-	-
9	LiCl	3.50	82.1	0.02	0.48	1.10	42.90	23,700	170

[a] data of transesterification oligomers taken from Table 3; [b] calculated by HPLC after 145 min of transesterification

Reference

[1] F. L. Bi, Z. H. Xi, L. Zhao, *Int. J. Chem. Kinet.* **2018**, *50*, 188-203.

[2] P. H. Che, F. Lu, X. Nie, Y. Z. Huang, Y. L. Yang, F. Wang, J. Xu, *Chem. Commun.* **2015**, *51*, 1077-1080.

[3] S. Chatti, G. Schwarz, H. R. Kricheldorf, *Macromolecules* **2006**, *39*, 9064-9070.

[4] S. Chatti, H. R. Kricheldorf, G. Schwarz, *J. Polym. Sci., Part A: Polym. Chem.* **2006**, *44*, 3616-3628.

[5] J. Wu, P. Eduard, L. Jasinska-Walc, A. Rozanski, B. A. J. Noordover, D. S. V. Es, C. E. Koning, *Macromolecules* **2012**, *46*, 384-394.

[6] M. Zhang, W. Q. Lai, L. L. Su, Y. Lin, G. Z. Wu, *Polym. Chem.* **2019**, *10*, 3380-3389.

[7] M. Zhang, W. Q. Lai, L. L. Su, G. Z. Wu, *Ind. Eng. Chem. Res.* **2018**, *57*, 4824-4831.

[8] F. Fenouillot, A. Rousseau, G. Colomines, R. Saint-Loup, J. P. Pascault, *Prog. Polym. Sci.* **2010**, *35*, 578-622.

[9] M. Garaleh, T. Yashiro, H. R. Kricheldorf, P. Simon, S. Chatti, *Macromol Chem Phys* **2010**, *211*, 1206-1214.

[10] S. Chatti, M. A. Hani, K. Bornhorst, H. R. Kricheldorf, *High Perform. Polym.* **2009**, *21*, 105-118.

[11] W. J. Yoon, K. S. Oh, J. M. Koo, J. R. Kim, K. J. Lee, S. S. Im, *Macromolecules* **2013**, *46*, 2930-2940.

[12] Y. S. Eo, H. W. Rhee, S. Shin, *J. Ind. Eng. Chem.* **2016**, *37*, 42-46.